

Study of the Mechanism of the Reaction ${}^4\text{He}(e, e'p){}^3\text{H}$

J. F. J. van den Brand,^{(1),(a)} H. P. Blok,^{(1),(2)} H. J. Bulten,⁽¹⁾ R. Ent,^{(1),(2),(b)} E. Jans,⁽¹⁾ G. J. Kramer,⁽¹⁾
 J. M. Laget,⁽⁴⁾ J. B. J. M. Lanen,⁽³⁾ L. Lapikás,⁽¹⁾ J. S. Roebbers,⁽¹⁾ R. Schiavilla,^{(4),(c)}
 G. van der Steenhoven,⁽¹⁾ and P. K. A. de Witt Huberts⁽¹⁾

⁽¹⁾*Nationaal Instituut voor Kernfysica en Hoge Energifysica (NIKHEF-K),
 Postbus 4395, 1009 AJ Amsterdam, The Netherlands*

⁽²⁾*Department of Physics and Astronomy, Vrije Universiteit, Amsterdam, The Netherlands*

⁽³⁾*Fysisch Laboratorium, Rijksuniversiteit Utrecht, Utrecht, The Netherlands*

⁽⁴⁾*Département de Physique Nucléaire, Centre d'Etudes Nucléaires de Scalay, 91191 Gif-sur-Yvette CEDEX, France*

(Received 30 August 1990)

A serious breakdown of the distorted-wave impulse approximation has recently been observed in the proton-knockout reaction ${}^4\text{He}(e, e'p){}^3\text{H}$. In the phenomenological description of the data, charge-exchange contributions were included through a coupled-channel calculation. New data obtained in a wide range of kinematical configurations are presented in order to study the anomaly in more detail. Its magnitude and dependence on momentum transfer are well accounted for by a newly presented microscopic description of various interaction effects, including meson-exchange currents and charge-exchange processes.

PACS numbers: 25.30.Fj, 24.10.Eq, 25.10.+s, 27.10.+h

Knockout of a single proton from complex nuclei by high-energy electrons is generally assumed to proceed predominantly via a one-step reaction. In this description the virtual photon couples directly to the charge and the magnetic moment of the proton that is ejected and subsequently detected in coincidence with the scattered electron. Indications of deviations from this impulse-approximation (IA) ansatz have recently been reported in $(e, e'p)$ experiments involving light- and medium-heavy nuclei.¹⁻⁵ These authors tested the validity of the IA by determining the ratio R of transverse to longitudinal structure functions, which are related to the electromagnetic current and charge operators of the bound proton. Below the two-particle emission threshold deviations from IA predictions are found to be relatively small ($\leq 10\%$ near the top of the quasielastic peak), whereas above the threshold large anomalies have been observed.^{3,5} Several mechanisms have been proposed to account for the observed enhanced ratio of transverse and longitudinal structure functions. Most of them are based on strong-interaction effects on the ejected proton⁶⁻⁸ in the final state or on a conceptually novel hypothesis concerning the identity of protons bound in a dense many-body quantum system, i.e., medium-modified nucleon form factors.^{9,10} Furthermore, attempts have been made to explain the observed deviations from the IA in terms of the charge-exchange process,¹¹ i.e., neutron knockout via $(e, e'n)$ followed by a (n, p) charge-exchange reaction. However, this effect turns out to be relatively small [(1-2)% for the structure-function ratio R] for ${}^{12}\text{C}$ and ${}^{40}\text{Ca}$. At this moment a precise explanation of the observations is not available.

In a recent ${}^4\text{He}(e, e'p){}^3\text{H}$ experiment¹² a much larger discrepancy (40%) was observed between the data and

the results of a distorted-wave impulse-approximation (DWIA) calculation with an isospin-dependent optical potential. A possible explanation is that the charge-exchange process is larger in quasifree proton knockout from ${}^4\text{He}$, because of the $(N-Z)/A$ dependence of the isospin-dependent part of the optical potential (Lane potential¹³). To investigate this phenomenon in more detail we have extended the ${}^4\text{He}(e, e'p){}^3\text{H}$ experiment to parallel, antiparallel, and nonparallel kinematics. Here, the transferred momentum \mathbf{q} , the momentum of the outgoing proton \mathbf{p}_x , and consequently the missing momentum $\mathbf{p}_m = \mathbf{q} - \mathbf{p}_x$ are (anti-) parallel or nonparallel. This is the first experimental study of the $(e, e'p)$ reaction where such special kinematics are selected in order to probe the different contributions to the reaction mechanism. Cross sections have been measured as a function of momentum transfer, and of the proton-triton center-of-mass energy. In this Letter a microscopic model developed by Laget will be used for the description of the ${}^4\text{He}(e, e'p)$ reaction mechanism, and the results compared to both previously published data and the new data.

In Refs. 14 and 15 a model is discussed which describes the electrodisintegration process of ${}^3\text{He}$. This model has been recently extended¹⁶ to ${}^4\text{He}$ and involves the numerical calculation of various overlap integrals of the initial and final states of the process. The threebody and fourbody variational wave functions needed to calculate these overlap integrals were taken from a variational Monte Carlo calculation by Schiavilla *et al.*¹⁷ using the Argonne V14 nucleon-nucleon (NN) potential and the Urbana model-VII three-nucleon interaction. Since it was found that the use of the Urbana V14 NN potential leads to a slope of the nucleon momentum distribution in

^4He that is in better agreement with the data, we discuss in this Letter the results for the Urbana V14 NN potential. These have been obtained by multiplying the predictions for the Argonne NN potential with the ratio of both p - ^3H momentum densities¹⁶ at each missing momentum (in the momentum range covered by this experiment this scaling is of the order of 10%). Meson-exchange-current (MEC) contributions and NN -rescattering processes (in first order) have been included in the microscopic model. Since the virtual photon interacts with both protons and neutrons the charge-exchange process is also included in this calculation. This particular process will turn out to be an important element of the model in the comparison with the data.

We first discuss the results of the microscopic calculation for the previously measured data.¹² They were obtained at an incident electron energy of 425.6 MeV at the NIKHEF-K electron-scattering facility¹⁸ using a cryogenic target.¹⁹ The data shown in Fig. 1 were taken under two different kinematical configurations, with the total kinetic energy T_{pt} of the proton-triton pair in the center-of-mass system kept constant at 75 MeV. In the first kinematics (I) the electron-scattering angle $\theta_e = 70^\circ$, the virtual-photon polarization $\epsilon = 0.48$, and the transferred three-momentum $|\mathbf{q}| = 431$ MeV/ c . For the second kinematics (II) one has $\theta_e = 36^\circ$, $\epsilon = 0.80$, and $|\mathbf{q}| = 250$ MeV/ c . The dotted curve shows the plane-wave impulse-approximation (PWIA) result. In an earlier analysis¹² of this experiment the data were compared to a coupled-channel calculation (DWIA/CCIA) which employed the Lane formalism to include the charge-exchange process. No spin dependence was included in the isospin-dependent potential terms. A 40% discrepancy remained between the ratio of the theoretical and ex-

perimental values for kinematics I and II. The solid curves in Fig. 1 correspond to the results of the present microscopic model that includes final-state interactions (FSI), charge-exchange, and meson-exchange-current effects. The kinematics-I data, taken very close to the top of the quasielastic peak, are fairly well described by the theory. Here, the contribution of the transverse photon-nucleon coupling to the cross-section is sizable ($\theta_e = 70^\circ$), and the combined effect of (n,p) charge exchange and meson exchange compensates half of the reduction due to proton rescattering. For kinematics II (data taken in the high- ω tail of the quasielastic peak, where ω represents the energy transfer to the nucleus) the results of the calculation underestimate the data by about 20%. At high missing momenta the curve shows a flattening off that is not present in the data. This is presumably due to strong interference in a region where the PWIA term is of the same order of magnitude as the terms connected with proton rescattering and charge exchange. A major limitation of the microscopic calculation is that only a single NN rescattering is considered, whereas when the FSI effects are calculated with an optical-model potential, one accounts in a phenomenological manner for all possible rescattering processes of the outgoing protons. It remains to be investigated whether a better agreement with the data is obtained when higher-order rescattering effects are taken into account. Nevertheless, the results of the microscopic model are in better agreement with the data than the previous results of the coupled-channel calculation that includes charge exchange in a phenomenological manner.¹² The fact that the CCIA is less successful may be related to an oversimplified treatment of the charge-exchange process with a Lane potential, which has no spin dependence, or to the use of the mean-field approximation for the optical-model potential in the case of the ^4He nucleus, or to deficiencies in the specific optical-potential²⁰ parameters that were used. In particular, the isospin-dependent terms of the optical potential are poorly known for the energy region under consideration. Recently,²¹ fair agreement was found between the data and the results of a similar calculation using the same phenomenological optical potential²⁰ and a parametrization of the scarce charge-exchange data. It was shown that contributions from two-body charge and current operators and orthogonality corrections are important in the description of the data. However, an important factor of uncertainty in this calculation is associated with the sensitivity of the results to the optical potential.

In order to study the effects of the various contributions to the $(e,e'p)$ reaction cross section in greater detail, additional $^4\text{He}(e,e'p)^3\text{H}$ measurements have been performed at an incident electron energy of 425.6 MeV, where T_{pt} was varied in the range 31–107 MeV. The missing-momentum acceptance was centered at 100 MeV/ c in kinematical configurations where the missing-

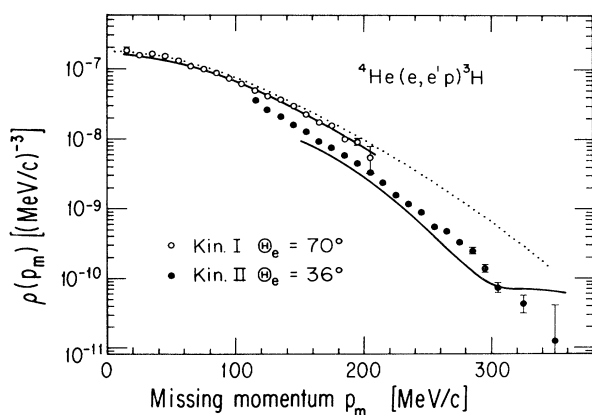


FIG. 1. Proton momentum distribution for the two-body breakup of ^4He . The error bars include the statistical error only. The dotted curve represents a PWIA calculation (Ref. 17) for the Urbana NN potential. The solid curves represent the results of the microscopic calculations (Ref. 16) taking FSI, charge-exchange, and MEC effects into account.

TABLE I. Experimental parameters for the ${}^4\text{He}(e,e'p){}^3\text{H}$ study of reaction-mechanism effects using parallel and antiparallel kinematics. Here \mathbf{k}' is the scattered electron momentum and θ_x the angle of the knocked-out proton.

$T_{pt}^{c.m.}$ (MeV)	$ \mathbf{k}' $ (MeV/c)	θ_e (deg)	$ \mathbf{p}_x $ (MeV/c)	θ_x (deg)	$ \mathbf{q} $ (MeV/c)	ϵ
32.0	351	63.88	313	-48.89	416	0.55
61.8	335	38.09	361	-51.09	262	0.79
62.0	306	93.31	434	-34.30	538	0.30
101.5	285	62.19	484	-40.15	385	0.54

momentum vector was directed either parallel or antiparallel to the transferred three-momentum. In these kinematical configurations the three-momentum transfer varied in the range $261 < |\mathbf{q}| < 534$ MeV/c. The kinematics are given in Table I. Details of the analysis are given in Ref. 12. The data obtained in the approximately 30-MeV/c-wide missing-momentum range are fitted with an exponential function. The cross section for each kinematics is represented by the value of this fit function at the maximum of the experimental phase space, i.e., at $|\mathbf{p}_m| = 100$ MeV/c. Its error was obtained from the full covariance matrix for the fit parameters and includes the 6% systematical error. In Fig. 2 the experimental results, which vary considerably depending on the kinematical configuration of the experiment, are shown in comparison with the calculations. The dotted curve gives the PWIA result, in which only the coupling of the virtual photon to the proton was taken into account. The results of the microscopic calculation with proton rescattering

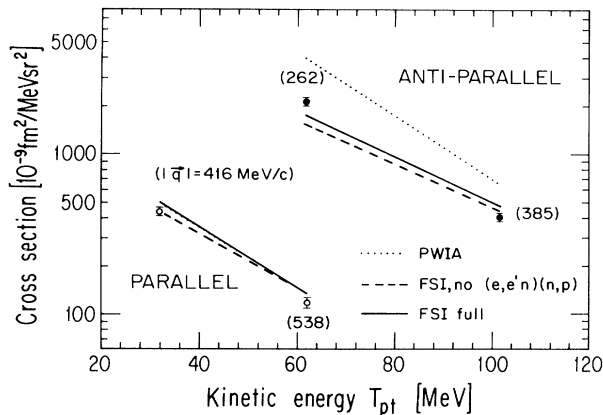


FIG. 2. The experimentally observed dependence of the five-fold differential cross section on the total hadronic kinetic energy for the reaction ${}^4\text{He}(e,e'p){}^3\text{H}$ measured at $p_m = 100$ MeV/c in parallel (open circles) and antiparallel (solid circles) kinematical configurations. The curves represent the various results of the microscopic calculations. These calculations were restricted to the kinematical configurations used in the experiment and in order to guide the eye the results have been joined by lines.

TABLE II. Experimental parameters for the ${}^4\text{He}(e,e'p){}^3\text{H}$ study of reaction-mechanism effects at a constant three-momentum transfer of 400 MeV/c.

$T_{pt}^{c.m.}$ (MeV)	$ \mathbf{k}' $ (MeV/c)	θ_e (deg)	$ \mathbf{p}_x $ (MeV/c)	θ_x (deg)	ϵ
31.5	409	52.99	308	-60.17	0.66
56.7	384	53.99	380	-64.45	0.64
81.8	359	54.86	442	-58.72	0.63
107.0	334	55.58	498	-45.38	0.61

but without charge exchange are represented by the dashed curve in Fig. 2. The solid curve represents the full calculation including the $(e,e'n)(n,p)$ contribution. It is seen that inclusion of charge-exchange increases the cross section by about 10%. The contribution of MEC is negligible in these kinematics.

The inclusion of MEC and NN -rescattering processes requires the calculation of a six-dimensional integral¹⁵ that runs over the internal relative momentum of the two nucleons of the active pair and the momentum of their center of mass. The two other nucleons are treated as spectators. This allows one to compute in more detail all the transition form factors between the ${}^4\text{He}$ ground state and the p - ${}^3\text{H}$ scattering state. Because of the Q^2 dependence of these form factors, the nucleon-rescattering contribution is expected to decrease when the momentum transfer increases: This is exactly what the data show. The various interaction effects are small in parallel kinematics, since $|\mathbf{q}|$ is large ($416 < |\mathbf{q}| < 538$ MeV/c), and large in antiparallel kinematics, since $|\mathbf{q}|$ is small ($262 < |\mathbf{q}| < 385$ MeV/c). The two measurements at $T_{pt} = 61$ MeV are particularly illuminating in this respect.

Because the contributions due to charge exchange depend on the values of both ϵ and \mathbf{q} , a further check consists of performing an experiment at a constant value of these kinematic quantities. Such an experiment was carried out in kinematical configurations at $\epsilon \approx 0.64$ and $|\mathbf{q}| = 400$ MeV/c. The incident electron energy in this experiment was 481.7 MeV, while here also $|\mathbf{p}_m|$ was kept centered at 100 MeV/c. The kinematics of this experiment are given in Table II and the results are shown in Fig. 3. The figure shows that the charge-exchange contribution (corresponding to the difference between the dot-dashed and dashed curves) is maximum at low kinetic energy and improves the agreement with the data. Note that the $T_{pt} = 31.5$ MeV kinematics is located at the low- ω side of the quasielastic peak. The interference between rescattering and charge-exchange contributions brings the results in almost perfect agreement with the data (dot-dashed curve). For an approximately constant value of ϵ , the charge-exchange effects contribute in a different way at each value of T_{pt} . The inclusion of MEC effects in the calculation results in a

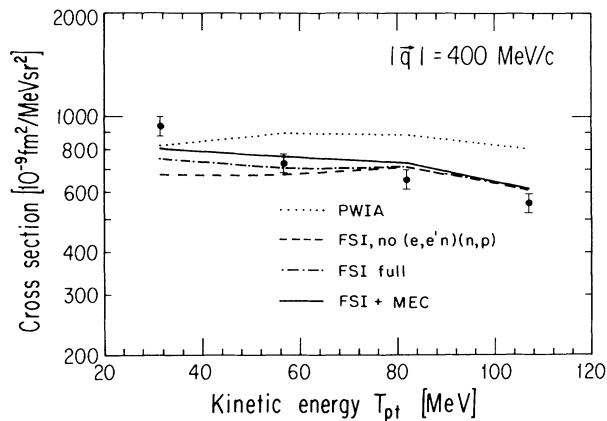


FIG. 3. The energy dependence of the fivefold differential cross section for the reaction ${}^4\text{He}(e, e'p){}^3\text{H}$ measured at $p_m = 100$ MeV/c at a fixed transferred three-momentum of 400 MeV/c. The curves connect the results of the various microscopic calculations.

further increase of (2–7)% of the cross section (solid curve).

In addition to the data presented above, a longitudinal-transverse separation of the ${}^4\text{He}(e, e'p){}^3\text{H}$ cross section has been performed at Saclay⁴ at $|\mathbf{p}_m| = 90$ MeV/c and three-momentum-transfer values ranging from 380 to 830 MeV/c. It has been found²² that the transverse structure function can correctly be described by the full microscopic calculation, but that the longitudinal part is overestimated by $\approx 15\%$. This latter conclusion seems to be at variance with the present results as the mainly longitudinal kinematics-II data of Fig. 1 are underestimated by the calculation. Additional longitudinal-transverse separation data on ${}^4\text{He}$ recently obtained at Saclay may clarify this situation.

In summary, it is concluded that a much improved description of the present data of the reaction ${}^4\text{He}(e, e'p){}^3\text{H}$ is obtained with a microscopic model that encompasses, in addition to the direct knockout contribution, proton-rescattering, charge-exchange, and meson-exchange processes. In the kinetic-energy region investigated in the present experiment the results of the microscopic model are in fair agreement with the data. On the one hand, the nucleon-rescattering contribution strongly decreases when the three-momentum transfer increases; on the other hand, the $(e, e'n)(n, p)$ two-step mechanism and the meson-exchange mechanisms contribute to the transverse structure function, where they cancel a part of

the reduction due to the proton-rescattering mechanisms. At present the reaction mechanism is described at the 15% level for a variety of kinematical configurations that cover the region from the low- ω side to the high- ω side of the quasielastic peak. This allows for an accurate extraction of the ${}^4\text{He}$ wave function.

This work is part of the research program of the National Institute for Nuclear Physics and High-Energy Physics (NIKHEF, section K), made possible by financial support from the Foundation for Fundamental Research on Matter (FOM) and The Netherlands' Organization for the Advancement of Scientific Research (NWO).

(a)Present address: Department of Physics, University of Wisconsin, Madison, WI 53706.

(b)Present address: Laboratory for Nuclear Science, Massachusetts Institute of Technology, Cambridge, MA 02139.

(c)Present address: Argonne National Laboratory, Argonne, IL 60439.

¹G. van der Steenhoven *et al.*, Phys. Rev. Lett. **57**, 182 (1986); **58**, 1727 (1987).

²D. Reffay-Pikeroen *et al.*, Phys. Rev. Lett. **60**, 776 (1988).

³P. E. Ulmer *et al.*, Phys. Rev. Lett. **59**, 2259 (1987).

⁴A. Magnon *et al.*, Phys. Lett. B **222**, 352 (1989).

⁵J. B. J. M. Lanen *et al.*, Phys. Rev. Lett. **64**, 2250 (1990).

⁶T. D. Cohen *et al.*, Phys. Rev. Lett. **59**, 1276 (1987).

⁷T. Suzuki, Phys. Rev. C **37**, 549 (1988).

⁸M. Kohno, Phys. Rev. C **38**, 584 (1988).

⁹L. S. Celenza *et al.*, Phys. Rev. Lett. **53**, 892 (1984).

¹⁰P. J. Mulders, Phys. Rev. Lett. **54**, 2560 (1985).

¹¹G. van der Steenhoven *et al.*, Phys. Lett. B **191**, 227 (1987).

¹²J. F. J. van den Brand *et al.*, Phys. Rev. Lett. **60**, 2006 (1988).

¹³A. M. Lane, Phys. Rev. Lett. **8**, 171 (1962).

¹⁴J. M. Laget, Phys. Lett. **151B**, 325 (1985).

¹⁵J. M. Laget, Phys. Lett. B **199**, 493 (1987).

¹⁶J. M. Laget, Nucl. Phys. A **497**, 391c (1989).

¹⁷R. Schiavilla *et al.*, Nucl. Phys. A **449**, 219 (1986).

¹⁸C. de Vries *et al.*, Nucl. Instrum. Methods Phys. Res. **223**, 1 (1984).

¹⁹J. F. J. van den Brand *et al.*, Nucl. Instrum. Methods Phys. Res. **261**, 373 (1987).

²⁰W. T. H. van Oers *et al.*, Phys. Rev. C **25**, 390 (1982).

²¹R. Schiavilla, Phys. Rev. Lett. **65**, 835 (1990).

²²J. M. Laget, "Physics with Polarized Beams and Polarized Targets," Proceedings of the Conference, Spencer, Indiana, October 1989, edited by J. Sowinski and S. Vigdor (World Scientific, Singapore, to be published).